

# UC Davis

## UC Davis Previously Published Works

### Title

A two-dimensional adsorption kinetic model for thermal hysteresis activity in antifreeze proteins

### Permalink

<https://escholarship.org/uc/item/8kj1p8tt>

### Journal

Journal of Chemical Physics, 124(20)

### ISSN

0021-9606

### Authors

Li, Q Z  
Yeh, Y  
Liu, J J  
[et al.](#)

### Publication Date

2006-05-01

Peer reviewed

## A two-dimensional adsorption kinetic model for thermal hysteresis activity in antifreeze proteins

Q. Z. Li

*The Theoretical Physics and Biology Laboratory, Department of Physics, College of Sciences and Technology, Inner Mongolia University, Hohhot 010021, China, and Department of Applied Science, University of California, Davis, California 95616*

Y. Yeh

*Department of Applied Science, University of California, Davis, California 95616*

J. J. Liu

*The Theoretical Physics and Biology Laboratory, Department of Physics, College of Sciences and Technology, Inner Mongolia University, Hohhot 010021, China*

R. E. Feeney

*Department of Food Science and Technology, University of California, Davis, California 95616*

V. V. Krishnan<sup>a)</sup>

*Department of Molecular, Cell, and Developmental Biology, University of California, Santa Cruz, Santa Cruz, California 95064, and Department of Applied Science and Center for Comparative Medicine, University of California, Davis, California 95616*

(Received 12 January 2006; accepted 16 February 2006; published online 23 May 2006)

Antifreeze proteins (AFPs) and antifreeze glycoproteins (AFGPs), collectively abbreviated as AF(G)Ps, are synthesized by various organisms to enable their cells to survive in subzero environments. Although the AF(G)Ps are markedly diverse in structure, they all function by adsorbing to the surface of embryonic ice crystals to inhibit their growth. This adsorption results in a freezing temperature depression without an appreciable change in the melting temperature. The difference between the melting and freezing temperatures, termed thermal hysteresis (TH), is used to detect and quantify the antifreeze activity. Insights from crystallographic structures of a number of AFPs have led to a good understanding of the ice-protein interaction features. Computational studies have focused either on verifying a specific model of AFP-ice interaction or on understanding the protein-induced changes in the ice crystal morphology. In order to explain the origin of TH, we propose a novel two-dimensional adsorption kinetic model between AFPs and ice crystal surfaces. The validity of the model has been demonstrated by reproducing the TH curve on two different  $\beta$ -helical AFPs upon increasing the protein concentration. In particular, this model is able to accommodate the change in the TH behavior observed experimentally when the size of the AFPs is increased systematically. Our results suggest that in addition to the specificity of the AFPs for the ice, the coverage of the AFPs on the ice surface is an equally necessary condition for their TH activity. © 2006 American Institute of Physics. [DOI: 10.1063/1.2186309]

### I. INTRODUCTION

Adaptation schemes for survival in extreme environments have resulted in the evolution of unique protein super-families that permit organisms to exist and thrive over a broad geographic distribution of the earth. In addition to the set of proteins that interact with biological solids in the biomineralization process, a class of proteins known as antifreeze proteins (AFPs) exists in low-temperature environments that inhibit lethal intra- or extracellular ice formation. AFPs and their glycosylated forms antifreeze glycoproteins (AFGPs), also known as thermal hysteresis proteins, play an important biochemical role in many animals,<sup>1,2</sup> insects,<sup>3-5</sup> and plants<sup>6</sup> that is a product of their cold adaptation pro-

cesses to defend their tissues from freezing injury. The solution of AFP exhibits a noncolligative freezing temperature depression that is from 300 to 500-fold effective compared with the equilibrium colligative depression observed for ordinary solutes (on a molar basis).<sup>7</sup> Extensive research in this area suggests that the mechanism for the freezing temperature depression of AFP is a result of its ice binding ability, which inhibits the growth of embryonic ice crystals that naturally emerge in supercooling water. This unique inhibitory function of AFP provides great potential for cryoindustrial usages, such as cryopreservation of tissues and cells and maintaining the texture of frozen materials.<sup>8-10</sup>

*In vitro*, the function of AFP is quantified using two observable effects due to presumed interaction of these proteins with ice: modification of the crystal growth morphology and thermal hysteresis (TH). Recently, Wathen *et al.*<sup>11</sup> have developed a model that combines three-dimensional (3D) mo-

<sup>a)</sup>Author to whom correspondence should be addressed. Electronic mail: vvkrisnan@ucdavis.edu

molecular representation and detailed energetic calculations of molecular mechanics techniques with a statistical probabilistic approach to study the inhibitory effects of AFPs on ice crystal formation. This modeling has produced results consistent with experimental observations, including the replication of ice-etching patterns, ice growth inhibition, and specific AFP-induced ice morphologies.<sup>11,12</sup> Although ice-surface recognition is undoubtedly crucial for AFP activity, it is not completely clear just how AFP-ice interaction is responsible for the phenomenon of TH. However, neither the computational methods described below nor conventional molecular dynamics studies of AFP-ice interactions<sup>13–16</sup> are able to completely explain the dynamic nature of TH; it is the hope that analyses such as that presented here will aid in experimental and modeling techniques that can provide insight into TH activity of the AFPs.

An early theoretical model for computing the thermal hysteresis of AF(G)P in solution is based on the Gibbs-Thomson (Kelvin) model.<sup>7,17</sup> It elegantly explains the non-colligative depression of AFP as an “adsorption-inhibition mechanism,” in which accumulations of AFPs onto the growing surfaces of ice crystals result in the creation of numbers of convex ice surfaces at the limited open spaces of ice between the bound AFPs.<sup>18,19</sup> The free energy of the convex ice surfaces becomes larger with the increase of the surface curvature. Therefore, further binding of water molecules onto the convex ice surfaces becomes energetically unfavorable, leading to the suppression of the ice crystal growth by increasing the number of bound AFPs. This irreversible ice binding model was then modified to a semireversible model<sup>20,21</sup> implying that the kinetics of AFP adsorption leads to ice growth inhibition. Li and co-workers have presented an analytical kinetic theory to estimate the TH as a function of the molar concentration of AFP and AFGPs.<sup>22–25</sup> Recently, Sander and Tkachenko<sup>26</sup> have proposed a “stones on a pillow” model in which the geometrical shape of the antifreeze molecule is used to explain the TH activity.

As AFPs tend to adopt different structural scaffolds,<sup>27–29</sup> the precise antifreeze mechanism for different kinds of AFPs adsorbing to ice crystals to inhibit ice growth is also expected to be different. For example, structure-based models developed for type I AFP ( $\alpha$ -helical structure) may not sufficiently explain the function of a  $\beta$ -helical AFP. The model should be able accommodate the fact that all the available sites on the surface of the ice lattice are expected to be indistinguishable and hence the AFP binding is “nonspecific.” It is important that the model should be general enough to accommodate the difference in the structural features while explaining the universal phenomenon of TH in all the AFPs and AFGPs. To incorporate all these features, we report a two-dimensional kinetic adsorption model, together with its initial application to the TH behavior of two AFPs. We find that this model is useful not only in understanding how changes in the protein concentration change the TH behavior, but also the recent experimental observation that alteration of the total size of AFPs affects their dynamic behavior. In addition to the binding of AFPs to ice surfaces, this model clearly suggests that the surface coverage of the proteins on ice is critical for their function.

## II. THE TWO-DIMENSIONAL ADSORPTION KINETIC MODEL

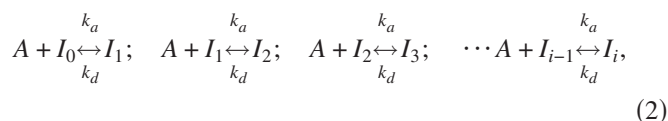
### A. Description of equilibrium kinetics of thermal hysteresis

Experimental studies performed in the field of AFP (AFGP) have yielded several characteristics indicating that these proteins adsorb to ice in a progressive manner. The kinetics of adsorption of AFPs to ice surfaces are expected to progress first by their attachment to the ice-water interface. This is then followed by rearrangement of adsorbed AFPs by diffusion, reorientation, and/or conformational change. The last of the steps is the detachment from the interface.<sup>20,21,30</sup> As AFPs do not interfere with the nucleation of ice crystals but somehow prevent their growth,<sup>7</sup> thermal hysteresis occurs in the presence of ice crystals which have already been seeded. AFPs will adsorb onto the surface of small ice crystals and interfere with the propagation of their growth, particularly on certain specific crystalline facets. As described by Strom *et al.*,<sup>31</sup> AFP-induced surface matching of periodic bond chains in two dimensions enables two-dimensional regular ice-binding surfaces of the insect AFPs to engage with the ice surfaces. This observation was originally reported by Wilson and Leader<sup>32</sup> and elaborated by Du and co-workers.<sup>33–35</sup>

We suppose that the interaction between the AFP and the surface of the ice crystal is a simple reversible adsorption process that may be represented by



where an AFP ( $A$ ) molecule with “ $i$ ” binding sites and ICE ( $I$ ) represents the appropriate crystal lattice of ICE to form the AFP bound of ice [ $A:I$ ]. This macroscopic equilibrium between the AFP and ICE is written in terms of several microscopic binding events given by



where  $I_0$  the bare ice lattice and antifreeze proteins ( $A$ ) adsorbed onto the ice surface  $I_i$  ( $i=1, 2, 3, \dots$ ), with the stepwise microscopic equilibrium constant, and  $K_i$  is then defined to be the ratio of on to off rates for each step. In the absence of cooperativity, each of the stepwise binding events will be equivalent, leading to  $K_1=K_2=K_3=\dots=K_i=K=k_a/k_d$  as assumed in writing Eq. (2).

The concentration of the adsorbed AFP can be expressed in terms of the products of stepwise equilibrium constant  $K_i$ , the concentration of the unbound AFPs, and the number of available sites on ice using the principle of mass action as

$$[I_1] = K_1[A][I_0]; \quad [I_2] = K_2[A][I_1]; \\ \cdots [I_i] = K_n[A][I_{i-1}]. \quad (3)$$

Rewriting Eq. (3) in terms of  $[I_0]$ ,

$$[I_i] = [A] \prod_{j=1}^i K_j [I_0]. \quad (4)$$

As in the case of AFP-ice system containing multiple identical binding sites and assuming that binding of an AFP molecule is independent of the others (no cooperativity), the stepwise binding constants are equal to the intrinsic association constant and the statistical factor determined by the number of microscopic states constituting different stages of AFP covered ice surface by the AFPs. This binding phenomenon is similar to the nonspecific binding of protein ligands to the periodically spaced minor/major grooves of a DNA molecule.<sup>36</sup> In general, an analytical isotherm modified from a Langmuir type of isotherm developed by McGhee and von Hippel is often used to study macromolecular binding equilibrium in which the surface of the substrate is modeled as an infinite one-dimensional lattice.<sup>37</sup> Because of the finite size of the ice crystals, the McGhee and von Hippel model does not readily permit the calculation of the statistical factors and the populations of the partially ligated states and one needs to resort to combinatorial methods. The product of  $K_i$  in Eq. (4) for “ $k$ ” bound AFPs can be written in general as

$$\prod_{i=1}^k K_i = C_k K^k, \quad (5)$$

where  $C_k$ 's are the statistical weights and these cause sequential decrease in the macroscopic binding constants with increasing saturation. Equations (4) and (5) therefore allow the estimation of the fraction of ice surface covered by AFPs.

The observed difference between the freezing and melting temperatures (thermal hysteresis activity) changes as a function of the amount of AFPs on the ice surface, which in turn is a function of the bulk AFP concentration.<sup>7</sup> Following the argument of Burcham *et al.*,<sup>38</sup> the fraction of sites covered (denoted as  $\theta$ ) therefore must be proportional to the observed thermal hysteresis activity. Consequently, the experimentally observed *plateau* must correspond to the lattice site saturation of the ice surface. If  $\Delta T$  is the difference between the melting and freezing temperatures of an AFP in solution and  $\Delta T_{\max}$  is the maximum observed thermal hysteresis activity (at saturation), for a specific AFP molecule then  $\theta$  can be formally written as

$$\theta = \frac{\Delta T}{\Delta T_{\max}}. \quad (6)$$

Therefore, for equilibrium measurement of AFP-ice interaction, with  $m$  AFP molecules adsorbing to  $N$  ice binding sites, using Eqs. (4) and (5) the coverage factor  $\theta$  can be written as

$$\theta = \frac{m}{N} \bar{C}_m, \quad (7)$$

where  $\bar{C}_m$  is the statistical factor providing the number of distinct ways for forming an ensemble of microscopic states for each of the  $m$  AFP molecules. Equating Eqs. (6) and (7) the observed thermal hysteresis is then written as

$$\Delta T = \theta \Delta T_{\max} = \left( \frac{m}{N} \bar{C}_m \right) \Delta T_{\max}. \quad (8)$$

By directly estimating the fraction of an ice surface covered by AFP ( $\theta$ ), this model can be used to estimate the observed difference in freezing and melting temperatures (the activity), as a function of the amount of AFP on the surface, which, in turn, is a function of the bulk AFP concentration. The fraction of sites covered  $\theta$ , therefore must be proportional to the observed activity, i.e., to thermal hysteresis.

## B. Analytic assessment of the fractional surface coverage

### 1. One-dimensional model

In order to determine  $\theta$ , we take the combinatorial approach. Analytical expressions for a one-dimensional lattice were originally given by Epstein<sup>39</sup> and have recently been reviewed by Munro *et al.*<sup>40</sup> Though we have extended the approach to a two-dimensional model that is more appropriate for the AFP binding to the ice surface, following the above-mentioned references, we briefly review the salient features of the one-dimensional model. We consider the case where the protein molecule (AFP) binds to “ $n$ ” but covers “ $m$ ” units of ice lattice (ICE), which is comprised of “ $N$ ” units (available binding sites on the ice surface). The interaction is governed by the intrinsic association constant  $K$ , which is the ratio of  $k_a$  and  $k_d$ , and governed by the equilibrium process described by Eq. (4). Therefore the fraction of the ice surface covered by AFP with concentration  $[A]$  [Eq. (7)] is rewritten in general terms as

$$\theta = \frac{m \bar{C}}{N}, \quad (9)$$

where  $\bar{C}$  is the average number of AFP molecules on  $N$  ice-lattice sites and is given by the molar ratio of bound AFP molecules to total available lattice sites on the ice and is written as

$$\bar{C} = \frac{\sum_{i=1}^R i C_i [I_i]}{(\sum_{i=0}^R C_i [I_i])}, \quad (10)$$

where  $R$  signifies an integer that is less than or equal to  $N/n$ , as the maximum number of AFP molecules which may bind to the lattice, and where  $C_i$  is the number of possible arrangements of the bound AFP molecules and empty available for distribution on the ice lattice, the statistical factor [see Eq. (5)]. Using Eqs. (9) and (10) the coverage factor  $\theta$  can be written as

$$\theta = \frac{\sum_{i=1}^R m i C_i [I_i]}{N (\sum_{i=0}^R C_i [I_i])}. \quad (11)$$

For a situation of a lattice consisting of  $N$  ice binding sites with sites with each AFP having  $n$  sites for binding, the number of possible places to distribute  $i$  AFP molecules will be  $N - ni$ . The total number of items to be arranged in the lattice can then be given by

$$C_i = \frac{(N - Mi + i)!}{(N - Mi)! i!}. \quad (12)$$

For example, with  $N=12$ ,  $n=4$ , and  $i=2$ , the number of configurations available [ $C_i$  from Eq. (12)] is 15. Physically this means that there is a total of 15 microscopic species that have two ( $i$ ) AFP proteins bound on the ice lattice, each having an intrinsic binding constant of  $K$ , while the macroscopic binding constant is a result of cumulative effect of the ensemble of such (15 here) species.

This combinatorial approach may be extended to include the possibility of the AFP occupying a total of  $m$  units which only binding to  $n$ . For this situation, the statistical weight can be given by<sup>40</sup>

$$C_i = \frac{(N - m(i-1)n + 1)!}{(N - m(i-1) - n + i)!}. \quad (13)$$

These expressions can be further extended to include cooperative binding<sup>40</sup> If  $i$  AFP molecules are bound, then various possible arrangements contain a maximum of  $i-1$  such adjacencies and the number of possible arrangements is defined as the number of ways of attaching  $i$  ligands with  $j$  adjacencies as

$$C_i = \sum_{j=0}^{i-1} C_{i(j)} \omega^j, \quad (14)$$

where

$$C_{i(j)} = \frac{[N - m(i-1) - n + 1]!(i-1)!}{[N - m(i-1) - n - i + j + 1]!(i-j)!j!(i-j-1)!}, \quad (15)$$

and  $\omega$  is the cooperativity factor. Though no cooperativity is considered in rest of the analysis, Eq. (15) is provided for the sake of completeness and it reduces to Eq. (13) when  $\omega=1$  (no cooperativity).

The generalized one-dimensional model includes the effect of cooperative binding, in which the intrinsic binding constants are given by the factor  $\omega$ .<sup>41-44</sup> Cooperative binding considers the number of attachments to adjacent segments ( $j$ ) possible in a particular arrangement of AFPs on a linear lattice. Expressions for cooperative binding as well as those with end effects for one-dimensional model have been derived.<sup>39,40</sup> Figure 1(a) schematically shows one of the several possible combinations of binding of a set of AFP molecules, each with three binding sites, to a finite length of one-dimensional ice lattice. This model allows the distinction between the number of sites covered by the AFP molecule to the number sites it is bound, i.e., some sites covered by AFP molecule may not have AFP adsorbed to them. For an ice crystal that has a total of  $N$  sites, where each AFP molecule can cover  $m$  sites on the surface of ice crystal but binds only to  $n$  sites ( $m \geq n$ ), the fraction (the ratio of the number of sites covered by AFPs to the total number of sites on all ice crystal surfaces) of the ice surface covered by AFPs with concentration can be defined on the basis of Eqs. (4) and (11),

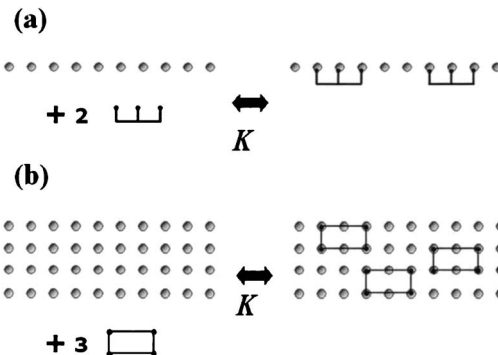


FIG. 1. Schematic representation of the (a) one- and (b) two-dimensional adsorption models. The AFP molecules bind to the ice lattice with an association constant  $K$ . The available sites on the surface of ice and on the AFP are given by large-gray and small-filled circles, respectively. In the two-dimensional representation of the model (b), the importance of AFPs to cover more sites than they bind to (here binds to four sites and covers 6) is highlighted.

$$\begin{aligned} \theta &= \frac{\sum_{i=1}^R mi C_i [I_i]}{N(\sum_{i=0}^R C_i [I_i])} = \frac{\sum_{i=1}^R mi C_i K^i [A]^i [I_0]}{N(\sum_{i=0}^R C_i K^i [A]^i [I_0])} \\ &= \frac{\sum_{i=1}^R mi C_i K^i [A]^i}{N(\sum_{i=0}^R C_i K^i [A]^i)}, \end{aligned} \quad (16)$$

where  $[A]$  is the concentration of AFP molecules ( $C_{\text{AFP}}$ ),  $[I_0]$  the concentration of ice crystal unoccupied,  $[I_i]$  the concentration of ice crystal occupied by  $i$  AFP molecules, and  $K$  is the microscopic adsorption equilibrium constant.

## 2. Two-dimensional model

In order to account for the effect of the interaction of AFP with ice surface, here we present the extension to two dimensions. Figure 1(b) schematically depicts the situation where the squares represent the AFP while the lattice shows the set of possible adsorption sites on the surface of the ice (no distinction between the different planes is considered). Considering that the surface of ice crystals is composed by  $M'$  lines and  $N$  identical adsorption sites on each line, an AFP molecule can cover  $m'$  lines. We may calculate the number of ways of attaching  $i_a$  AFPs with  $j$  adjacencies in the  $a$ th line ( $a=1, 2, \dots, M'$ ) ( $M$  is an integer given by  $M'/m'$ ) in a manner similar to the one-dimensional model. If  $i_a$  AFP molecules are bound, the various possible arrangements contain a maximum of  $(i_a - 1)$  such adjacencies.

This can be achieved by rewriting the regression relations after replacing  $l$  by  $i_a$  in Eq. (15). This leads to the  $C_i$ 's for the two-dimensional model with cooperativity as

$$\begin{aligned} C_{i_a(j)} &= C_{i_a-j}^{N-m(i_a-1)-n+1} C_j^{i_a-1} \\ &= \frac{[N - m(i_a - 1) - n + 1]!(i_a - 1)!}{[N - m(i_a - 1) - n - i_a + j + 1]!(i_a - j)!j!(i_a - j - 1)!}. \end{aligned} \quad (17)$$

For noncooperative interactions ( $\omega=1$ ), the  $C_i$ 's for the two-dimensional model become [using Eq. (13) instead of Eqs. (15) and (9)]

$$C_{i_a} = \frac{[N - m(i_a - 1) - n + i_a]!}{[(N - m(i_a - 1) - n)! i_a!]}, \quad (18)$$

where the “ $a$ ” is an index that goes from 1 through  $M$ . In addition, if there are  $L$  lines, which have been occupied by AFP molecules among  $M'$  lines, the number of ways of attaching  $L$  lines of AFP to the ice should be

$$P_{M'} = \frac{(L + M' - Lm')!}{L!(M' - Lm')!}. \quad (19)$$

Therefore, in the attachment of the  $i_1 + i_2 + \dots + i_{M-1} + i_M$  AFP molecules to two-dimensional lattice comprising of  $M'$  lines and  $N$  identical adsorption sites on each line, and the number of possible arrangements is

$$P_{M'} C_{i_1} C_{i_2} \dots C_{i_M}. \quad (20)$$

Here  $M$  is the integer value of the  $M'/m'$ , and  $L$  is the number of lines adsorbed by AFP molecules, which can be calculated recursively. In the two-dimensional model [Fig. 1(b)], the surface of ice crystal is composed of  $M'$  lines with  $N$  same adsorption sites on line. Furthermore, an AFP molecule can cover  $m'$  lines and  $m$  sites in the same line. By extending the one-dimensional model, the fraction of the ice crystal surface covered by AFPs with concentration  $[A]$  (the ratio of the number of sites covered by AFPs to the total number of available sites on all ice crystal surfaces) can be derived from the one-dimensional expression by replacing each point  $i$  by the line  $i_a$ . After rearranging, the coverage factor ( $\theta$ ) for the two-dimensional model becomes

$$\theta = \frac{\sum_{i_1, i_2, \dots, i_M=0}^R mm' (i_1 + i_2 + \dots + i_M) P_{M'} C_{i_1} C_{i_2} \dots C_{i_M} (K[A])^{(i_1 + i_2 + \dots + i_M)}}{NM' (\sum_{i_1, i_2, \dots, i_M=0}^R P_{M'} C_{i_1} C_{i_2} \dots C_{i_M} (K[A])^{(i_1 + i_2 + \dots + i_M)})}. \quad (21)$$

Now using the argument to correlate the coverage factor to the thermal hysteresis and using Eqs. (6)–(8) and (16) the expression for  $\Delta T$  becomes

$$\Delta T = \theta \Delta T_m = \frac{\sum_{i_1, i_2, \dots, i_M=0}^R mm' (i_1 + i_2 + \dots + i_M) P_{M'} C_{i_1} C_{i_2} \dots C_{i_M} (K[A])^{(i_1 + i_2 + \dots + i_M)}}{NM' (\sum_{i_1, i_2, \dots, i_M=0}^R P_{M'} C_{i_1} C_{i_2} \dots C_{i_M} (K[A])^{(i_1 + i_2 + \dots + i_M)})} \Delta T_m. \quad (22)$$

For a given  $\Delta T_m$ , the thermal  $\Delta T$  can be estimated by calculating  $\theta$ . Here  $\theta$  was calculated using computer code written in C++ on a desktop windows machine (available from the authors upon request). Though, it is straightforward to code for  $\theta$ , in a computer program, proper book keeping of the various indices is necessary and the calculation becomes computer intensive as the number of sites (ice and AFP) increases.

### III. RESULTS

We apply the two-dimensional model to two different kinds of AFPs that are structurally repetitive: (a) *Tenebrio molitor* AFP (TmAFP) and (b) *Choristoneura fumiferana* AFP (CfAFP).

The TmAFP produced by the beetle is a right-handed  $\beta$ -helix comprised of 12-amino acid repeats that stack to form a rectangular “box” with an array of Thr residues on the surface.<sup>45,46</sup> The distance between Thr residues in the array matches the spacing of oxygen atoms in the ice lattice, and the Thr array has been demonstrated to be the ice-binding face of the protein.<sup>5,47</sup> Recently, Marshall *et al.*<sup>48</sup> have made use of the extreme regularity of these proteins to explore systematically the relationship between antifreeze activity and the area of the ice-binding site. Each of the 12-amino acid contains disulfide-bonded central coils of the TmAFP a Thr- $X_n$ -Thr ( $X_n$  stands for other aminoacids) ice binding motif. By adding coils to, and deleting coils from, the seven-coil parent antifreeze protein, a series of constructs with

6–11 coils has been made. There was from 10- to 100-fold gain in activity upon going from six to nine coils, depending on the concentration that was compared. Analysis of TH activity as a function of concentration demonstrates that the activity of TmAFP constructs changes dramatically with the number of coils.<sup>48</sup> The repetitive structure of TmAFP provides an ideal opportunity to investigate the relationship between the size and the activity of an AFP.

Figures 2 and 3 show the application of the two-dimensional adsorption model to TmAFP following the nomenclature given in the original experimental work by Marshall *et al.*<sup>48</sup> Naturally occurring forms are referred to as wild types 4–9 (w.t. 4–9, wild type), while those where coils are deleted or added are referred to as minus or plus, respectively. The total number of different AFPs is 6. These are labeled with increasing size as minus 1, w.t. 4–9 (natural protein), plus 1, plus 2, plus 3, and plus 4. Figure 2 shows the plot of the TH activity for all six proteins [panels (a) through (f)]. Symbols in Fig. 2 are the experimental values, while the continuous curves are the calculations based on Eq. (15). Figure 3(a) shows the ribbon diagram of all six proteins (generated using lzzg.pdb<sup>5</sup>), and Fig. 3(b) shows the TH temperature at a protein concentration of 60  $\mu$ M with the dark bars representing the values obtained from the model, and the gray bars experimental results reproduced from reference.<sup>48</sup>

In generating the theoretical results, with no loss of generality we assumed  $N$  and  $M'$  [rows and columns of the

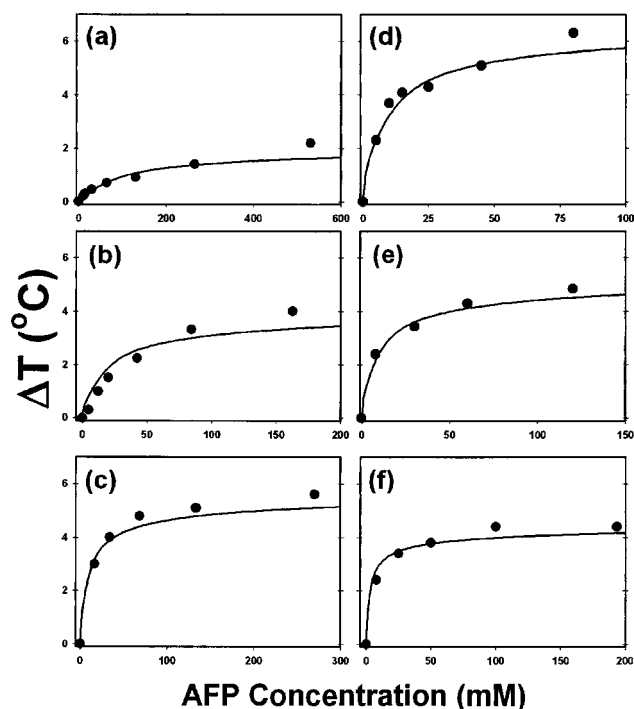


FIG. 2. Plot of the thermal hysteresis activity ( $\Delta T$ ) determined by the adsorption model for the various constructs of TmAFP and its comparison with the corresponding experimental values, as function of TmAFP concentration. (a) TmAFP minus-1 coil, (b) wild type 4–9, (c) plus-1 coil, (d) plus-2 coils, (e) plus-3 coils, and (f) plus-4 coils. The continuous lines are the predicted dynamics while the symbols are represent the experiments (Ref. 46). The activity is maximum for TmAFP plus-2 coils and tapers off as additional coils are introduced.

two-dimensional ice lattice, see Fig. 1(b)] to vary from 20 to 200 and from 3 to 60, respectively. In order to produce the best fit to the experimental data, we use as much experimental information as possible on the initial choice of the various indices and are listed in Table I. For the experimental values of TmAFP,<sup>48</sup> we obtain  $\Delta T_m$  and  $K$  as 2.6 °C and  $1.6 \times 10^{-3}$  (minus 1), 5.0 °C and  $6.3 \times 10^{-3}$  (w.t. 4–9), 6.5 °C and  $15 \times 10^{-3}$  (plus 1), 7.8 °C and  $15 \times 10^{-3}$  (plus 2), 6.0 °C and  $15 \times 10^{-3}$  (plus 3), and 5.0 °C and  $15 \times 10^{-3}$  (plus 4), respectively. The number of effective adsorption sites ( $n$ ) for each of the TmAFPs is obtained from the crystal structure<sup>5</sup> and the detailed analyses of the ice-binding surface.<sup>49,50</sup> This leads to  $n=5$  for minus 1 and  $n=6$  for the rest of the AFPs. The numbers of sites covered ( $m$ ) are 6, 8, 10, 12, and 10 for minus 1, w.t. 4–9, plus 1, plus 2 and plus 3 (also plus 4), respectively. The number of lattice lines along the second dimension ( $m'$ ) is assumed to be 3 for all the proteins. We have also assumed that  $N=60$ ,  $M'=15$ , and the cooperativity constant  $\omega=1$ . When these values are used along with the actual experimental concentration, we are able to generate curves that fit the experimental results of Fig. 2. The same numbers were used for generating the theoretical results in Fig. 3, in which the AFP concentration was fixed to be at 60  $\mu\text{M}$ .

Figure 4 shows the application of the two-dimensional adsorption model to CfAFP and Table I also lists the choice of the various indices used to obtain the best fit to experimental results. Filled circles and squares show experimental

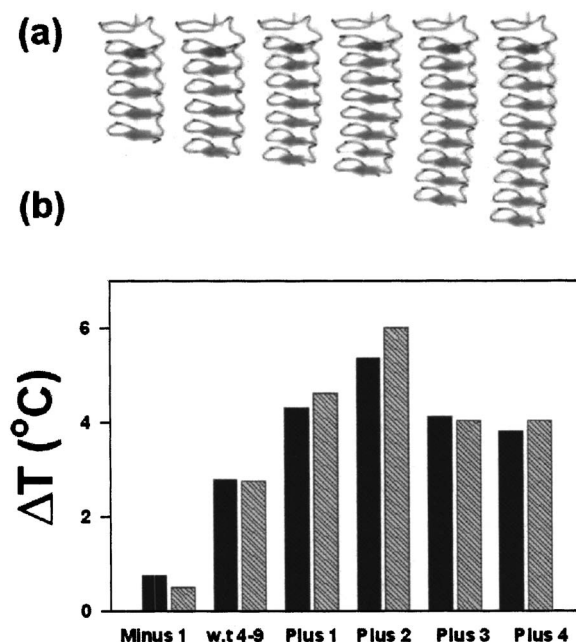


FIG. 3. Comparison of the adsorption model predicted  $\Delta T$  and the corresponding experimental values of the various TmAFP constructs at a protein concentration of 60  $\mu\text{M}$ . (a) Ribbon diagram of the three-dimensional structure of the various TmAFP constructs. (b) Theoretically predicted (dark bars) vs experimental values (gray bars) of  $\Delta T$  for the various TmAFP constructs.

values from the two different protein constructs, CfAFP-337 and CfAFP-501, respectively. CfAFP is a left-handed  $\beta$ -helix composed of tandem 15-amino acid imperfect repeats that form a triangular cross section and present a regular array of Thr residues on a flat  $\beta$  sheet on the surface of the protein.<sup>5,49</sup> CfAFP has several isoforms and all of them have the Thr–X–Thr motifs, repeated every 15 amino acids. Here we apply our model to generate the most studied isoforms of CfAFP, CfAFP-337, and CfAFP-501.<sup>49,50</sup> CfAFP-337 has a molecular weight of 9 kD and has been extensively studied by NMR spectroscopy and x-ray crystallography.<sup>29</sup> CfAFP-501 contains a 30 residues insertion on the CfAFP-337 and has about 66% sequence similarity with CfAFP-337. The TH

TABLE I. AFP-ice adsorption parameters for TmAFP and CfAFP.

Antifreeze protein		$\Delta T_m$ (°C) <sup>a</sup>	$K$ ( $\times 10^{-3}$ ) <sup>b</sup>	$n$ <sup>c</sup>	$m$ ( $m'$ ) <sup>c</sup>
TmAFP <sup>d</sup>	Minus 1	2.6	1.6	5	6(3)
	w.t. 4–9	5.0	6.3	6	8(3)
	Plus 1	6.5	15	6	12(3)
	Plus 2	7.8	15	6	10(3)
	Plus 3	6.0	15	6	12(3)
	Plus 4	5.0	15	6	10(3)
CfAFP <sup>e</sup>	337	4.2	8.0	6	8(3)
	501	7.2	15	6	12(3)

<sup>a</sup> $\Delta T_m$  values were obtained from experimental measurements (Ref. 48).

<sup>b</sup> $K$  values (intrinsic binding equilibrium constants) for adjusted for a best fit to the experimental values.

<sup>c</sup> $n$ ,  $m$ , and  $m'$  values and other values ( $N=60$ ,  $M'=15$ , and  $\omega=1$ ) were chosen to fit the AFP-ice binding topology of the respective proteins (see text).

<sup>d</sup>TmAFP: *Tenebrio molitor* antifreeze protein.

<sup>e</sup>CfAFP: *Choristoneura fumiferana* antifreeze protein.

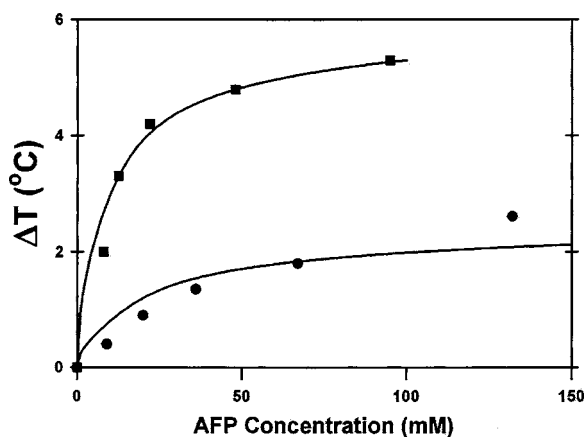


FIG. 4. Plot of the thermal hysteresis activity ( $\Delta T$ ) determined by the adsorption model for the two different CfAFP constructs and its comparison with the corresponding experimental values, as function of protein concentration. Experimental values for CfAFP-337 and CfAFP-501 are shown by filled circles and squares (Ref. 50), respectively, and the corresponding theoretical predictions are shown by continuous curves.

activity for both these proteins is experimentally available.<sup>50</sup> The 30 amino-acid insert in CfAFP-501 forms two additional loops within its highly regular  $\beta$ -helical structure. CfAFPs, such as TmAFPs, are ideal for model validation, since they too have a two-dimensional Thr array on one face of the protein that forms the ice-binding site.<sup>50</sup>

According to the experimental data, the maximum observed activities  $\Delta T_m$  and the adsorption equilibrium constant  $K$  are 2.2 °C and  $8 \times 10^{-3}$ , respectively for CfAFP-337, while these values are 7.2 °C and  $15 \times 10^{-3}$ , respectively, for CfAFP-501. Based on the experimental results we further determined the number of effective adsorption sites ( $n$ ) as 6 for both CfAFP-337 and CfAFP-501. The numbers of sites covered by one AFP molecule ( $m$ ) are taken as 8 and 12 for CfAFP-337 and CfAFP-501, respectively. The remaining parameters ( $m'$ ,  $N$ , and  $M'$ ) are taken to have the same values as those associated with TmAFPs. These parameters, used along with Eq. (15), lead to the continuous curves of Fig. 4. CfAFP-501 has higher activity than CfAFP-337, because of the increase in the number of  $\beta$ -helical segments. This observation is similar to increased activity of TmAFP with increase in the number of  $\beta$ -helical segments (*vide supra*).

#### IV. DISCUSSION

Overall, the two-dimensional adsorption model is in good agreement with thermal hysteresis measurements involving  $\beta$ -helical AFPs. In particular, the model reproduces the  $\Delta T$  values for different lengths of the protein in both TmAFP and CfAFP. It demonstrates that the increased activity is due mainly to increased size of the protein and more importantly, the model fits well with the fact that for larger molecular weight TmAFPs (plus 3 and 4); the relative TH activity tapers off due to decrease in the AFP-specific surface coverage. These results suggest that the size of the ice-binding face of CfAFP is an important determinant of its antifreeze activity.<sup>50</sup> As the length of the helix increases, the overall protein flexibility also increases. Given the regularity of ice lattice, too much flexibility on the part of AFP might

have detrimental effects on AFP-ice interaction. Therefore, the effective length will be a compromise or a delicate balance between the ice-binding area and structural flexibility. These findings parallel those where a longer isoform of the  $\alpha$ -helical fish type I AFP, containing four ice-binding repeats as compared with the usual three, were found to be a more potent antifreeze protein.<sup>51</sup>

The development of the new two-dimensional model and its application to a set of AFPs suggest two important aspects on the function of AFPs: (a) AFPs' recognition of the ice surface with affinity and specificity is an important first step in their function. (b) The phenomenon of thermal hysteresis depends on the effective surface covered by AFP in addition to the actual number of adsorption sites. The exact nature of the interaction is determined by the fundamental molecular recognition processes of AFPs for ice through a set of adsorption sites, e.g., hydrogen bonding, while the surface coverage is determined by other factors such as molecular shape, effective surface area, and dynamics. This observation is consistent with the results of TmAFP. Here, for the plus-1 proteins, the number of adsorption sites and the surface coverage are optimal for producing the maximum  $\Delta T$ . When the size of the protein is increased to plus 3 and plus 4, though the number of adsorption sites is increased, the total surface coverage is reduced due to the increase in the dynamic nature of the larger protein.

The covered ice surface plays a key role in increasing antifreeze activity. This result is in agreement with the experimental conclusion obtained by producing recombinant analogs of the linked dimer that assess the effects of protein size and the number and area of the ice-binding site(s).<sup>52</sup> There is increasing evidence showing that antifreeze activity can be enhanced by increasing the length/area of the ice-binding site. The type I AFP9 isoform from winter flounder serum at 52 amino acids in length (4.3 kDa) has an extra 11-amino acid repeat compared with a common serum isoform, HPLC-6, and therefore has a larger ice-binding face.<sup>53</sup> On the other hand, it is interesting that the ratio of the maximum activities for  $\beta$ -helical TmAFP and CfAFP is approximately equal to the ratio of the ice crystal area covered by them. This result is in good coincidence with the viewpoint of Baardsnes *et al.*<sup>52,53</sup> In addition, although there is much difference in antifreeze activity for  $\beta$ -helical AFPs, the difference in the number of their ice-binding sites is small as compared to the large difference in TH activity. This result is consistent with the recent experimental results on partitioning of fish and insect antifreeze proteins into ice.<sup>11,48</sup> A new model for simulating 3D crystal growth for the study of antifreeze proteins suggests that the degree of AFP activity results more from AFP ice-binding orientation than from AFP ice-binding strength. Altering AFP off rates did not significantly change the pattern of distribution on the ice surface. Furthermore, artificially increasing the TmAFP off rate by a factor of 2 (weakening AFP-ice adsorption) did not greatly reduce its ice inhibition effectiveness.<sup>11</sup> These results are consistent with our result that the number of adsorption sites is less than the number of sites covered by AFP. These results suggest that while ice-binding ability is a necessary prerequisite for AFP activity, the degree of antifreeze activity is not



determined by AFP ice-binding strength alone. More recently, by using of the semiempirical molecular orbital method, the correlation between the numbers of coils in TmAFP constructs and the AFP-ice interaction energy was systematically investigated. The result indicates that the interaction energy increases gradually as more coils are included, but then slows down and eventually reaches a plateau upon further increase of the number coils. Only for the first ~five coils, the increase in interaction energy corresponds well with the number of coils.<sup>12</sup>

In comparison with single site adsorption models (AFP molecule adsorbed on an ice surface only occupies an adsorption site), multisites adsorption model proposed here can incorporate the cooperative properties in the adsorption process of the low molecular weight AFP on the ice crystal surface.<sup>23</sup> In addition, the ice-binding sites on an AFP molecule as a whole cannot be separated from the adsorption process of AFP on the surface of ice crystal. The ice-adsorption sites on an AFP molecule are distributed on the two-dimensional surface for the  $\beta$ -helical TmAFP and CfAFP. Based on these experimental results for the  $\beta$ -helical TmAFP and CfAFP, we have considered the antifreezing mechanism of AFP to be mainly due to the surface coverage of the AFPs that results from the interaction of AFP two-dimensional adsorption to the ice crystal surface, and hence presented a two-dimensional adsorption model. According to the theory, we can calculate the thermal hysteresis activities of the  $\beta$ -helical TmAFP and CfAFP in solution, and our results suggest that the difference in antifreeze abilities results from the ice surfaces covered by AFP. Moreover, the current theoretical model can be extended to include the antifreeze action of both AFPs and AFGPs in general, as well as the effect of cooperativity.

*Note added in proof:* Since the acceptance of this manuscript, Liu and Li [Chem. Phys. Lett. **422**, 67 (2006)] have presented a two-dimensional homogeneous lattice model based on the extension of McGhee and von Hippel's one-dimensional model.<sup>37</sup> This model has been applied to explain the thermal hysteresis in type I AFP.

## ACKNOWLEDGMENTS

The authors thank Professor W.H. Fink and Professor Y. Duan for many discussions and S.P. Mielke for critical reading of the manuscript. This work was supported by National Natural Science Foundation of China [30160025 for two of the authors (Q.Z.L. and J.J.L.)].

<sup>1</sup> P. L. Davies and B. D. Sykes, *Curr. Opin. Struct. Biol.* **7**, 828 (1997).

<sup>2</sup> C. B. Marshall, G. L. Fletcher, and P. L. Davies, *Nature (London)* **429**, 153 (2004).

<sup>3</sup> J. G. Baust, R. R. Rojas, and M. D. Hamilton, *Cryo-Letters* **6**, 199 (1985).

<sup>4</sup> C. A. Knight and J. G. Duman, *Cryobiology* **23**, 256 (1986).

<sup>5</sup> S. P. Graether, M. J. Kuiper, S. M. Gagne, V. K. Walker, Z. Jia, B. D. Sykes, and P. L. Davies, *Nature (London)* **406**, 325 (2000).

<sup>6</sup> M. E. Urrutia, J. G. Duman, and C. A. Knight, *Biochim. Biophys. Acta* **1121**, 199 (1992).

<sup>7</sup> Y. Yeh and R. E. Feeney, *Chem. Rev. (Washington, D.C.)* **96**, 601 (1996).

<sup>8</sup> J. F. Carpenter, T. Arakawa, and J. H. Crowe, *Dev. Biol. Stand.* **74**, 225 (1992).

<sup>9</sup> H. Chao, P. L. Davies, and J. F. Carpenter, *J. Exp. Biol.* **199**, 2071 (1996).

<sup>10</sup> L. M. Hays, R. E. Feeney, L. M. Crowe, J. H. Crowe, and A. E. Oliver, *Proc. Natl. Acad. Sci. U.S.A.* **93**, 6835 (1996).

<sup>11</sup> B. Wathen, M. Kuiper, V. Walker, and Z. Jia, *J. Am. Chem. Soc.* **125**, 729 (2003).

<sup>12</sup> K. Liu, Z. Jia, G. Chen, C. Tung, and R. Liu, *Biophys. J.* **88**, 953 (2005).

<sup>13</sup> A. Wierzbicki, M. S. Taylor, C. A. Knight, J. D. Madura, J. P. Harrington, and C. S. Sikes, *Biophys. J.* **71**, 8 (1996).

<sup>14</sup> A. Wierzbicki, J. D. Madura, C. Salmon, and F. Sonnichsen, *J. Chem. Inf. Comput. Sci.* **37**, 1006 (1997).

<sup>15</sup> J. D. Madura, K. Baran, and A. Wierzbicki, *Anat. Clin.* **13**, 101 (2000).

<sup>16</sup> D. H. Nguyen, M. E. Colvin, Y. Yeh, R. E. Feeney, and W. H. Fink, *Biopolymers* **75**, 109 (2004).

<sup>17</sup> J. A. Raymond and A. L. DeVries, *Proc. Natl. Acad. Sci. U.S.A.* **74**, 2589 (1977).

<sup>18</sup> C. A. Knight, C. C. Cheng, and A. L. DeVries, *Biophys. J.* **59**, 409 (1991).

<sup>19</sup> C. A. Knight and A. Wierzbicki, *Cryst. Growth Des.* **1**, 439 (2001).

<sup>20</sup> C. L. Hew and D. S. C. Yang, *Eur. J. Biochem.* **203**, 33 (1992).

<sup>21</sup> D. Y. Wen and R. A. Laursen, *J. Biol. Chem.* **267**, 14102 (1992).

<sup>22</sup> J. J. Liu and Q. Z. Li, *Chem. Phys. Lett.* **378**, 238 (2003).

<sup>23</sup> Q. Z. Li and L. F. Luo, *Chem. Phys. Lett.* **216**, 453 (1993).

<sup>24</sup> Q. Z. Li and L. F. Luo, *Chem. Phys. Lett.* **223**, 181 (1994).

<sup>25</sup> Q. Z. Li and L. F. Luo, *Chem. Phys. Lett.* **320**, 335 (2000).

<sup>26</sup> L. M. Sander and A. V. Tkachenko, *Phys. Rev. Lett.* **93**, 128102 (2004).

<sup>27</sup> M. M. Harding, L. G. Ward, and A. D. J. Haymet, *Eur. J. Biochem.* **264**, 653 (1999).

<sup>28</sup> M. M. Harding, P. I. Anderberg, and A. D. J. Haymet, *Eur. J. Biochem.* **270**, 1381 (2003).

<sup>29</sup> S. P. Graether and B. D. Sykes, *Eur. J. Biochem.* **271**, 3285 (2004).

<sup>30</sup> L. Chapsky and B. Rubinsky, *FEBS Lett.* **412**, 241 (1997).

<sup>31</sup> C. S. Strom, X. Y. Liu, and Z. Jia, *Biophys. J.* **89**, 2618 (2005).

<sup>32</sup> P. Wilson and J. Leader, *Biophys. J.* **68**, 2098 (1995).

<sup>33</sup> N. Du and X. Y. Liu, *Appl. Phys. Lett.* **81**, 445 (2002).

<sup>34</sup> N. Du, X. Y. Liu, and C. L. Hew, *J. Biol. Chem.* **278**, 36000 (2003).

<sup>35</sup> X. Y. Liu and N. Du, *J. Biol. Chem.* **279**, 6124 (2004).

<sup>36</sup> C. R. Cantor and P. R. Schimmel, *Biophysical Chemistry: The Behavior of Biological Macromolecules* (Freeman, New York, 1980), Part III.

<sup>37</sup> J. D. McGhee and P. H. von Hippel, *J. Mol. Biol.* **86**, 469 (1974).

<sup>38</sup> T. S. Burcham, D. T. Osuga, Y. Yeh, and R. E. Feeney, *J. Biol. Chem.* **261**, 6390 (1986).

<sup>39</sup> I. R. Epstein, *Biophys. Chem.* **8**, 327 (1978).

<sup>40</sup> P. D. Munro, C. M. Jackson, and D. J. Winzor, *J. Theor. Biol.* **203**, 407 (2000).

<sup>41</sup> R. C. Kelly, D. E. Jensen, and P. H. von Hippel, *J. Biol. Chem.* **251**, 7240 (1976).

<sup>42</sup> D. E. Jensen, R. C. Kelly, and P. H. von Hippel, *J. Biol. Chem.* **251**, 7215 (1976).

<sup>43</sup> I. R. Epstein, *Biopolymers* **18**, 2037 (1979).

<sup>44</sup> S. C. Kowalczykowski, L. S. Paul, N. Lonberg, J. W. Newport, J. A. McSwiggen, and P. H. von Hippel, *Biochemistry* **25**, 1226 (1986).

<sup>45</sup> Y. C. Liou, A. Tocilj, P. L. Davies, and Z. Jia, *Nature (London)* **406**, 322 (2000).

<sup>46</sup> M. E. Daley, L. Spyropoulos, Z. Jia, P. L. Davies, and B. D. Sykes, *Biochemistry* **41**, 5515 (2002).

<sup>47</sup> C. B. Marshall, M. E. Daley, L. A. Graham, B. D. Sykes, and P. L. Davies, *FEBS Lett.* **529**, 261 (2002).

<sup>48</sup> C. B. Marshall, M. E. Daley, B. D. Sykes, and P. L. Davies, *Biochemistry* **43**, 11637 (2004).

<sup>49</sup> E. K. Leinala, P. L. Davies, and Z. Jia, *Rev. Esp. Otorinolaringol. Neurocir.* **10**, 619 (2002).

<sup>50</sup> E. K. Leinala, P. L. Davies, D. Doucet, M. G. Tyshenko, V. K. Walker, and Z. Jia, *J. Biol. Chem.* **277**, 33349 (2002).

<sup>51</sup> H. Chao, R. S. Hodges, C. M. Kay, S. Y. Gauthier, and P. L. Davies, *Protein Sci.* **5**, 1150 (1996).

<sup>52</sup> J. Baardsnes, M. J. Kuiper, and P. L. Davies, *J. Biol. Chem.* **278**, 28942 (2003).

<sup>53</sup> J. Baardsnes, L. H. Kondejewski, R. S. Hodges, H. Chao, C. Kay, and P. L. Davies, *FEBS Lett.* **463**, 87 (1999).